Journal of the Optical Society of Korea, Vol. 3, No. 1, March 1999, pp. 10-14

Characterization of Doped Silicon from 0.1 to 2.5 THz Using Multiple Reflection

Tae-In Jeon

Department of Electrical Engineering, Korea Maritime University, Dongsam-dong, Yeongdo-ku, Pusan 606-791, KOREA

E-mail: jeon@hanara.kmaritime.ac.kr

(Received January 12, 1999)

Via THz Time domain spectroscopy, the characterization of high conductive n-type, 1.31 Ω cm silicon can be measured by directly analyzing the multiple reflections using Fabry-Perot theory. The magnitude and phase difference of total transmission show good agreement between theoretical and experimental values over a 2.5 THz frequency range with complex index of refraction and power absorption. The measured absorption and dispersion are strongly frequency-dependent, and all of the results are well fit by a Cole-Davidson type distribution.

I. INTRODUCTION

The frequency-dependent complex conductivity of doped silicon is one of its most important technical properties. However, due to the difficulty of reaching the THz frequency region with conventional sources, many scientists have studied the dynamics of carriers in silicon by microwave techniques [1,2]. Microwave techniques can probe only low frequencies, but the strongest absorption of the free carriers and change in index of refraction lie between 0.1 THz and 2 THz. For reliable characterization of commercially important silicon, the dynamics of carriers must be investigated in the frequency range from 0.1 THz to 2 THz. This result was obtained with a repetition rate of 87 MHz and an average power of 10nW in the THz beam of Ref.6.

In this research, the measured silicon has high conductivity. Because high conductivity semiconductors have extremely high power absorption, the semiconductor samples must be a very thin to transmit the THz pulse. However, due to the thin sample, the output THz pulse has multiple reflections which are responsible for the oscillations in the frequency-dependent transmission of the sample. In order to remove the multiple reflections, the sample was replaced by an identical cylinder of high resistivity float zone (FZ) Si or to avoid the multiple reflection problem, reflection THz time-domain spectroscopy (THz-TDS) measurements are used [4]. In this research, the characterization of doped Si can be measured by directly analyzing the multiple reflection THz pulses. The multiple reflection measurement is the first time application to the complex conductivity of doped Si from low frequencies to frequencies higher than the plasma frequency and the carrier damping rate.

II. EXPERIMENTAL SETUP

THz-TDS is based on the optoelectronic generation and reception of a beam of subpicosecond THz pulses. High-performance optoelectronic sources [5] have been used to generate and detect short pulses of THz radiation. Such a THz optoelectronic system is illustrated in Figure 1(a). A GaAs transmitting antenna with a simple coplanar transmission line geometry and a silicon on sapphire (SOS) receiving antenna are both optoelectrically driven by 6 mW average power of 70 fs pulses from a mode-locked Ti:sapphire laser. The antennas are micron size dipoles embedded in a coplanar transmission line. Because the optoelectronic receiver is gated synchronously with the excitation of the transmitter, the two paths between the beamsplitter and the receiver chip should be the same length. The THz pulse is obtained by scanning the relative time delay between the laser excitation pulse and the laser detection pulse. When the measurement delay line is stepped to measure the data, the manual delay line is fixed. The manual delay line is used only to optimize the THz signal while adjusting the THz system. In order to eliminate the effects of water vapor on the THz beams [6], the THz system is located in an airtight dry box.

The THz-TDS is shown in Figure 1(b). THz pulses are optoelectronically generated by the ultrashort laser pulses incident on the optoelectronic transmitter chip. The generated THz beam is collimated by a silicon lens, which is attached to the back of the source chip

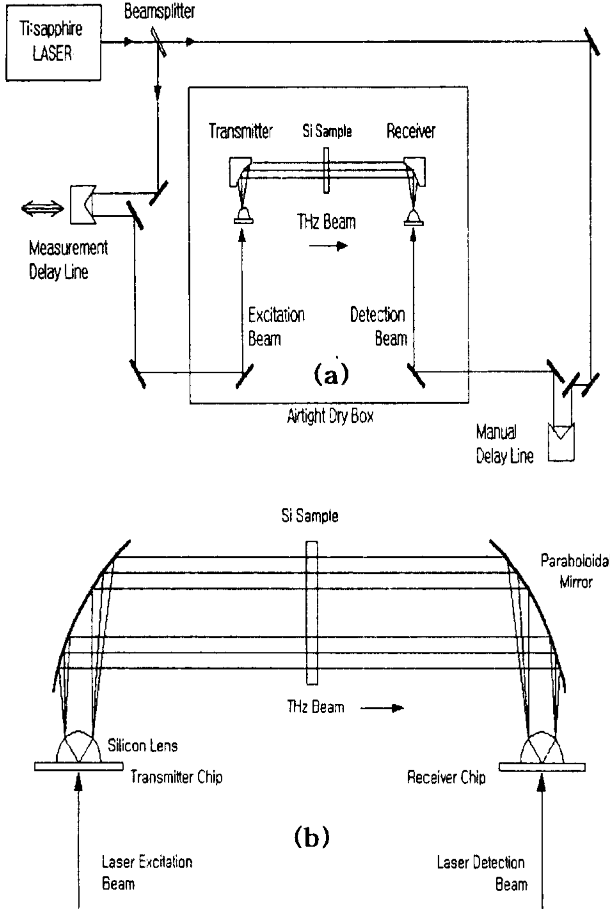

FIG. 1. (a) Schematic diagram of the experimental setup. (b) Schematic diagram of the optoelectronic THz beam system.

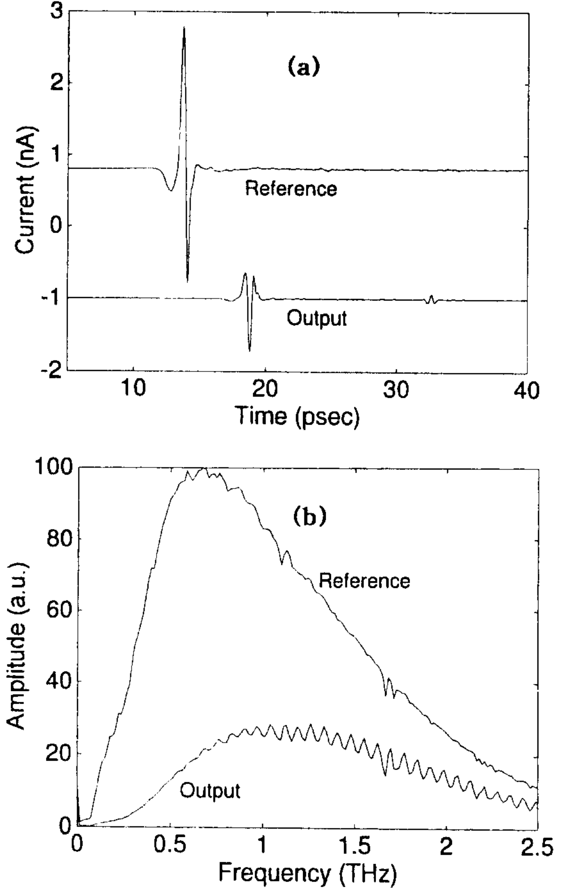

FIG. 2. (a) Measured reference and output THz Pulses. (b) Comparison of two spectra; reference and output.

and whose front surface is located at the focus of the paraboloidal mirror. The collimated THz beam propagates and diffracts to the paraboloidal mirror, where the THz radiation is recollimated into a highly directional beam with beam diameters proportional to the wavelength. This combination of the paraboloidal mirror, silicon lens, and the optoelectronic THz source chip forms the THz transmitter. A second identical paraboloidal mirror and silicon lens combination on the receiving end focuses the THz beam on the detector and forms the THz receiver.

III. MEASUREMENTS

A THz pulse propagating in n-type, 1.31 Ω cm 600 μm-thick silicon will be reshaped due to the absorption and dispersion of the Si sample. These changes can be dramatic and are quantified by comparing the transmitted pulse to the reference pulse, as demonstrated by the measurements presented in Figure 2(a). The upper figure in Figure 2(a) is the reference THz pulse and the lower figure in Figure 2(a) is the output THz pulse after transmission through the Si sample. The amplitude of the output pulse is reduced about 70% compared to that of the reference pulse. The output pulse amplitude and shape are changed due to reflection loss, frequency-dependent absorption, and dispersion of the sample. The second transient is the THz pulse reflected inside of the thin sample. In the output THz pulses the position of the main pulse is 19.0 psec and the position of the first reflected THz pulse is 32.7 psec. Multiple reflections are responsible for the oscillations in the corresponding amplitude related spectrum shown in Figure 2(b).

The absorption of the thin sample is influenced by interference effects. The transmission equation of the thin sample has already been described by Fabry-Perot theory [7,8]. The total transmission of a free standing absorptive thin Si sample at normal incidence is given by [7]

$$t_{tot} = \frac{t_{12}t_{23}\exp(-\alpha d/2)\exp(i\beta_0)}{1 + r_{12}r_{23}\exp(-2\alpha d)\exp(i2\beta_0)} \tag{1}$$

where α is an absorption coefficient, and $\beta_0 = 2\pi n_2 d/\lambda_0$. λ_0 is the free space wavelength and d is thickness of sample. The reflection and transmission

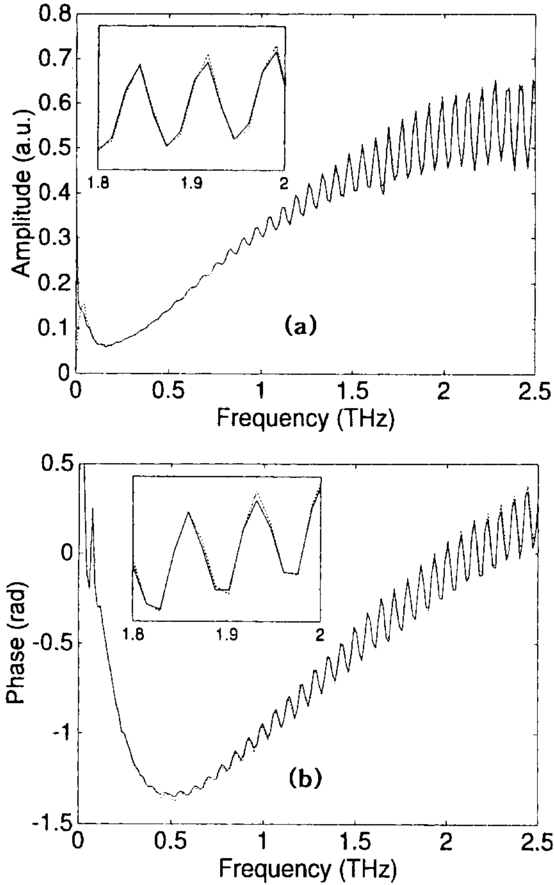

FIG. 3. (a) The measurement (Solid line) and theory (Dashed line) of the magnitude of total transmission. (b) The measurement (Solid line) and theory (Dashed line) of the phase difference.

coefficients r and t are $r_{12} = (n_1 - n_2)/(n_1 + n_2)$, $r_{23} = (n_2 - n_3)/(n_2 + n_3)$, $t_{12} = 2n_1(n_1 + n_2)$, and $t_{23} = 2n_2(n_2+n_3)$ where n_1, n_3 are indices of refraction of air and n_2 is the index of refraction of the Si sample. In this case $n_1 = n_3$ and $r_{12} = -r_{23}$. The absorption coefficient and indices of refraction of the Si sample can be determined by fitting Equation (1) to the measured oscillation values. Figure 3(a) shows the magnitude of the total transmission. The inset shows details from 1.8 THz to 2 THz. The solid line is obtained by taking the measured spectrum with the sample (output) divided by the spectrum without the sample (reference), and the dashed line is calculated from the theory of Equation (1). These two lines are in good agreement thoughout the entire frequency range. Because of the multiple reflections, the phase change is strongly frequency-dependent. The measured phase difference is the combination of the phase change caused by the sample and phase shift due to the multiple reflections. To compare the theoretical phase shift with the measured extra phase shift, the phase differences are numerically adjusted to around 0 rad. These relations are shown in Figure 3(b). The solid line is the measured phase term and the dashed line is the theoretical phase term. The two lines agree quite well. Therefore, the fitted absorption coefficient and index of refraction curves are reasonable values. In these figures, the frequency and amplitude of the oscillation depend on the thickness of the sample and the index of refraction of the sample.

The frequency-dependent complex dielectric constant is equal to the square of the complex index of refraction $n = n_r + in_i$. The imaginary index n_i is determined by measuring the power absorption coefficient $\alpha = 4\pi n_i/\lambda_0$. The dielectric response for doped silicon is described by the following general relationship [1,9]:

$$\varepsilon = \varepsilon_{si} + i\sigma/(\omega\varepsilon_0) \tag{2}$$

where ε_{si} is the dielectric constant of undoped Si, σ is the complex conductivity, and ε_0 is the free-space permittivity. The index of refraction $n_r = 3.417$ and absorption coefficient $\alpha \approx 0$ have been measured [10] for undoped silicon over the frequency range discussed in this paper. Associated with the conductivity, the key parameters characterizing the dynamics of the free carriers in semiconductors are plasma frequency ω_p, and the carrier damping rate $\Gamma = 1/\tau$ where τ is the carrier collision time. The plasma frequency ω_p is given by $\omega_p^2 = Ne^2/(\varepsilon_0 m^*)$ where $m^* = 0.26\ m_0$ for effective electron mass and $m^* = 0.37\ m_0$ for the effective hole mass; m_0 is the free-electron mass. N is number density of carriers density. The theoretical approach discussed in this paper is described by the equation [3]

$$\sigma = \varepsilon_0\omega_p^2\tau/(1 - i\omega\tau)^\beta \tag{3}$$

where β is a distribution parameter limited to values between 0 and 1. For Drude theory $\beta = 1$ in Equation (3). The Cole-Davidson (C-D) distribution used here is given by Equation (3), which appears as the complex conjugate of the C-D distribution from Debye theory [11–14]. The dc conductivity is given by $\sigma_{dc} = e\mu N$, with mobility $\mu = e/(\Gamma m^*)$ for Drude and Cole-Davidson. The fitting parameters are given in Table 1, together with the corresponding number densities and mobilities.

The power absorption of the sample is shown in Figure 4(a). The solid oscillating line is the measurement

TABLE 1. Theoretical fitting parameters for the measurements presented in Fig.4.

Parameters	Drude	C-D
$\omega_p/2\pi$	0.935 (THz)	0.873 (THz)
$\Gamma/2\pi$	0.635 (THz)	0.55 (THz)
β	1	0.89
N	2.8×10^{15} (cm^{-3})	2.5×10^{15} (cm^{-3})
μ	1700 $(cm^2/Vsec)$	1960 $(cm^2/Vsec)$

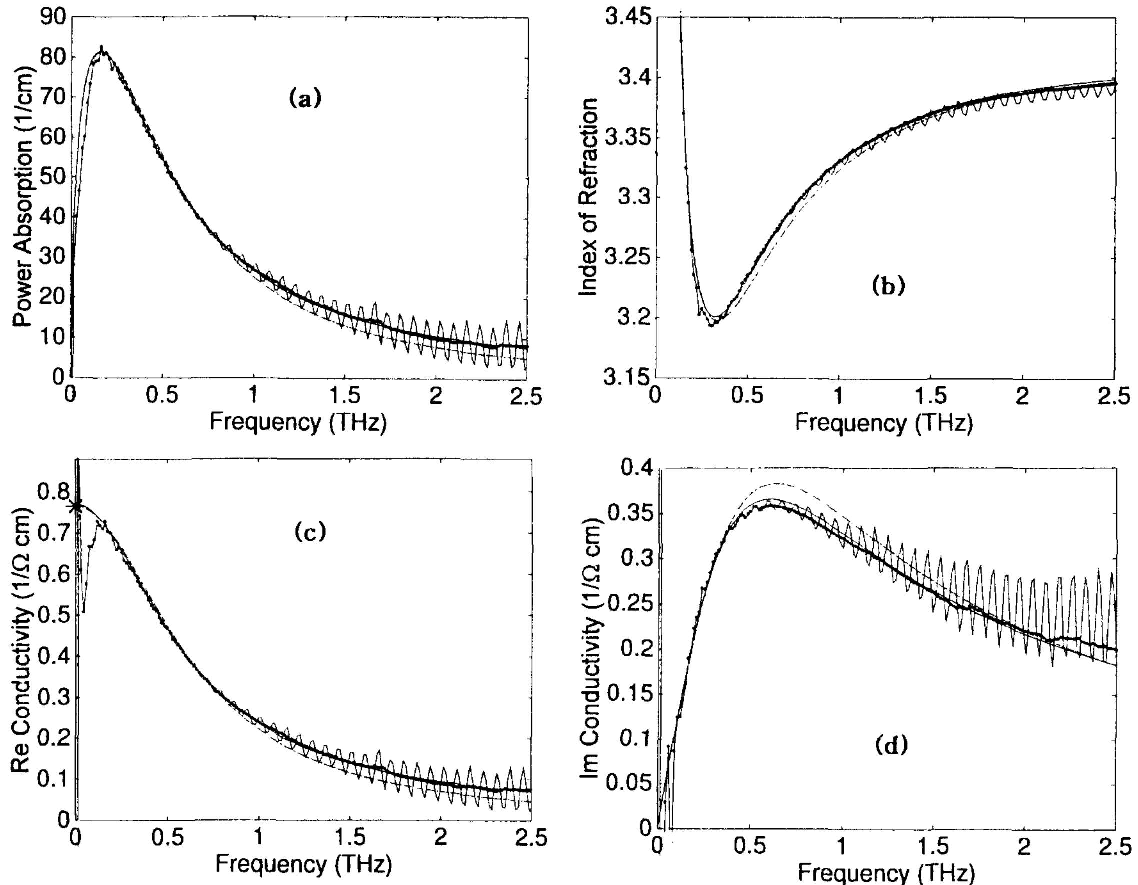

FIG. 4. Measurements and theoretical comparisons; measurement (Solid oscillating line), fitting curve (Dotted line), Drude theory (Dashed line), and Cole-Davidson distribution (Solid non-oscillating line). (a) Power absorption. (b) Index of refraction. (c) Real conductivity. (d) Imaginary conductivity.

and the dotted line is a curve fitting to the measurement. Also, the dashed line describes simple Drude theory and the solid non-oscillating line describes the C-D distribution. Only the C-D line agrees very well [3] with the fitted curve. The measured indices of refraction plotted in Figure 4(b) show strong frequency dependences and well resolved minima that are only fitted by the C-D distribution. Given these measured absorptions and indices of refraction, Equation (3) determines the real σ_r and imaginary σ_i parts of the conductivity as shown in Fig. 4(c) and 4(d). At zero frequency(dc value), the four-point probe measurement is indicated by the asterisk in Fig. 4(c). The real part of the conductivity provides a good measure of σ_{dc} as evidenced by the agreement with the four-point probe measurement. Because all the fits originate from the same value at $\omega = 0$, the product μN is the same for the two theories.

IV. CONCLUSIONS

Using the technique of THz-TDS, the frequency-dependent absorption and dispersion of n-type Si was measured from 0.1 THz to 2.5 THz. The output THz pulses had multiple reflections because of the thin sample. The magnitude of total transmission and phase difference are strongly frequency-dependent, and this phenomena can be explained by Fabry-Perot theory. The measurements were in good agreement with the theoretical results. Therefore, the characterization of the thin Si sample can be measured by directly analyzing the multiple reflections. Compared to earlier studies of doped silicon [15], the new experimental results have a sufficient precision to test alternative theories. Drude theory fits well with the measurement for the lowest frequencies. However, as the frequency increases beyond the carrier damping rate, $\Gamma/2\pi$, the measured power absorption and real conductivity become significantly larger than those of the simple Drude theory, while the measured peak of the imaginary part, occurring approximately at $\Gamma/2\pi$, is significantly lower than the Drude result. All the measurements are exceptionally well fit by the Cole-Davidson distribution, which corresponds to Drude theory with a fractional exponent of the distribution parameter β.

ACKNOWLEDGMENTS

The author would like to acknowledge Dr. D. Grischkowsky of electrical and computer engineering in Oklahoma State University for use of the THz-TDS system.

REFERENCES

[1] R.T. Kinsaewitz and B. Sentizky, J. Appl. Phys. **54**, 3394 (1983).
[2] J.D. Holm and K.S. Champlin, J. Appl. Phys. **39**, 275 (1968).
[3] T.-I. Jeon and D. Grischkowsky, Phys. Rev. Lett. **78**, 1106 (1997).
[4] T.-I. Jeon and D. Grischkowsky, Appl. Phys. Lett. **72**, 2259 (1998); **72**, 3032 (1998).
[5] N. Katzenellenbogen and D. Grischkowsky, Appl. Phys. Lett. **58**, 222 (1991).
[6] M van Exter, Ch. Fattinger, and D. Grischkowsky, Opt. Lett. **14**, 1128, (1989).
[7] M. Born and E. Wolf, *Principle of Optics*, (Pergamon Press, Oxford, 1987).
[8] T. Kihara and K. Yokomori, Appl. Opt. **29**, 5069 (1990).
[9] T. Ohba and S. Ikawa, J. Appl. Phys. **64**, 4141 (1988).
[10] D. Grischkowsky, S. Keiding, M van Exter, and Ch. Fattinger, J. Opt. Soc. Am. B **7**, 2006 (1990).
[11] D.W. Davidson and R.H. Cole, J. Chem. Phys. **19**, 1484 (1951).
[12] S. Havriliak, Jr. and D.G. Watts, Polymer **27**, 1509 (1986).
[13] K. Pathmanathan and J.R. Stevens, J. Appl. Phys. **68**, 5128 (1990).
[14] G.A. Niklasson, K. Brantervik, and L. Borjesson, J. Non-Cryst. Solids **131**, 1096 (1991).
[15] M. van Exter and D. Grischkowsky, Phys. Rev. B **41**, 12140 (1990).